Supporting Information

Zeitlin et al. 10.1073/pnas.0908233106

SI Text

Laser Sample Preparation. For laser microirradiation experiments, cells were cultured in 35-mm glass-bottom dishes (Mattek catalog# P35G-1.5–14-C), coated by incubation with 10 μg/mL fibronectin in PBS (30–60′ at 37 °C). After coating, fibronectin was aspirated, and cells were plated in the presence of tetracycline 18–24 h before laser microirradiation.

Laser Induction of DNA Damage. A short-pulsed green wavelength Nd: YVO_4 laser (532 nm, repetition rate: 76 MHz, 12 ps; Vanguard Laser System, Spectra-Physics, Inc.) was used in these studies. The beam was expanded and relayed to the back aperture of the microscope objective (63×, NA = 1.4) via the epi-fluorescence port of the Zeiss inverted microscope (Axiovert 200). The pulse energy at the focused spot was varied by the orientation of a Glan-Thompson polarizer (mounted on a motorized rotational stage). After passing through the Glan-Thompson polarizer, the laser beam passed through the microscope to the back aperture of the microscope objective. Laser power at the back aperture of the objective was measured with a power meter/detector (S 120 UV, Thorlabs). The transmission of the Zeiss Plan-Neofluar 63×/1.4 NA objective was measured using the dual objective method to correct for total internal reflection losses at the objective-oil-glass-water interfaces, and determined to be 0.68.

The laser pulse energy at the object focal plane was determined by measuring the input energy at the back aperture of the objective multiplied by the transmission factor (0.68) of the objective. Exposure time in the focal spot was controlled by a computerized mechanical shutter. The exposure time of 30 ms represents an accumulation of 2.28×10^6 pulses (12 ps each) per focused spot of an area 0.17 μm^2. The scanning pattern of the focal spot in the nucleus was generated by a rapid scanning mirror (FSM-300, Newport Inc.), controlled by in-house software on a LabView platform and National Instrument's data acquisition and control board (2). From the measured power at the back aperture of the objective, individual 12 ps pulse energy in the focal spot was 0.098 nJ/pulse.

A series of control experiments were performed to determine the average laser power to consistently create detectable DNA damage. Low power (5.5 mW before objective) created DNA damage detected by immunofluoresence for H2AX and other damage markers in fixed cells [Fig. 1; (3)]. 11.2 mW was used as the maximum dose for cells expressing GFP-tagged proteins. In every experiment with GFP-tagged proteins, stable inducible GFP-CENP-A expressing cells were used to verify consistent frequency of focus formation at this dose.

The average power measured before the objective was 5.5, 11, and 16.5 mW. Thus, the average power after the objective was 3.75, 7.5, and 11.2 mW in the focused spot. Since the 63× (1.4 NA) microscope objective focuses the beam to a diffraction limited spot diameter of 464 nm, peak irradiances of 0.25×10^{10}, 0.49×10^{10}, and 0.735×10^{10} W/cm^2 were achieved in the focused spot. For one line scan of 5 μm (with ≈10 spots/line), 2,234.4 μJ of total energy (energy/pulse × no. of pulses per spot × no. of spots in the line) was delivered to each cell. We estimate that this amount of energy will create on average 1–10 breaks per targeted box.

Images were originally collected manually at varying intervals; longer movies later used a time-lapse parameter with regular collection frequency. Temporal resolution was thus limited by both the frequency of manual collection and the time required for laser targeting (typically 1–3 min per field, depending on the number of cells targeted). Timestamps are indicated for the images shown. Targeted areas were generally chosen to be located near or overlapping with nucleoli, to help ensure that laser exposure occurred internal to the nucleus.

Controlled Environment Stage Holder. A Basic Water Jacket microscope stage incubator (MSI) (Okolabhttp://www.okolab.com/182.page) was mounted on the Axiovert 200M Zeiss microscope for temperature control (37 °C, via water jacket) and CO_2 (injecting module for CO_2 and air mixture, 5% final CO_2).

CENP-A-GFP Stable Inducible Cell Line Construction and Induction. GFP-tagged CENP-A plasmid (gift from Kevin Sullivan, National University of Ireland, Galway) encoding GFP ligated to the amino terminus of human CENP-A (1), was cut with NheI and NotI, and the pcDNA5/FRT/TO plasmid (Invitrogen) was cut with *Kpn*I and *Not*I. A double-strand oligonucleotide adaptor (cat#15000, EZ Clone Systems) used to make the *Kpn*I site compatible with *Xba*I, was added directly to ligations (NEB Quick Ligase Kit). The final plasmid was verified by sequencing (Eton Bioscience) with BGH reverse and CMV promoter primers (Invitrogen).

Human Flp-In Hek293 cells (Invitrogen) were co-transfected with FRT recombinase plasmid pOGG4 and GFP-CENP-A in plasmid pcDNA5/FRT/TO, selected transiently for the recombinase with blasticidin (15 μg/mL), and maintained under selection for the GFP-CENP-A gene with 200 μg/mL hygromycin B. Colonies were isolated using glass cylinders, and expanded in selective media. Aliquots of low-passage cells from each clone were frozen; freshly thawed aliquots were used for 6–12 passages. GFP-CENP-A expression was induced with tetracycline (final concentration, 5 μg/mL).

RNA Preparation and Gene Expression Analysis. RNA (≈250 ng/μL final) was prepared from approximately 600,000 cells per sample, using Qiashredder and RNeasy (Qiagen). RNA was eluted in 30 μL nuclease-free water, and quantitated on a Nanodrop ND-1000 Spectrophotometer. cDNA was generated using 50 μL RNA at 60 ng/μL with the Applied Biosystems high-capacity cDNA archive kit. Taqman assays were performed on an Applied Biosystems Instrument 7000, in quadruplicate, normalized against actin RNA, and repeated twice. Quantitation curves (serial dilutions) were generated for all samples. Data were analyzed using Microsoft Excel and graphs were generated using CricketGraph.

Cellular Fractionation. GFP-CENP-A expressing cells were grown to confluence in 15-cm dishes with tetracycline for 24 h. Media was removed and cells were scraped into a 1.5-mL hypotonic buffer dish (1 mM EDTA, 20 mM HEPES, pH 7.4, 5 mM KCl, and 2 mM $MgCl_2$, with beta-mercaptoethanol and protease inhibitor mixture (Roche or Sigma). Nonidet P-40 (Igepal CA-630, Sigma) was added to a final concentration of 0.1% and cells were incubated on ice 10 min. To isolate nuclei, lysate was layered on a 50% sucrose cushion and spun, 1 min at 10,000 rpm in an Eppendorf tabletop minicentrifuge. The supernatant was taken (cytosolic fraction) and pellets were resuspended in the same hypotonic buffer (without Nonidet P-40) and spun through sucrose cushions twice more. The resulting nuclear pellet was resuspended in 75 μL nuclear extract buffer (hypotonic buffer + 5 M NaCl to 400 mM final concentration and 20% Triton X-100

to 1% final concentration). The sucrose cushion procedure was repeated three times as before, and the final pellet represents the chromatin fraction.

Transiently Transfected GFP-Tagged Expression Constructs. CENP-A:H3.1 chimeras and mutants were obtained in the original vectors (4), except H3.1^{CATD} (5). ORFs were amplified using PCR (Pfu Ultra High Fidelity, Stratagene cat#600380–52; with matching buffer and 10% DMSO). Oligonucleotide primers were designed to preserve the reading frame and linker from the GFP-CENP-A construct (N terminus), and to insert a stop codon to eliminate the C-terminal HA tags in the original vectors. PCR products were band purified (USA Scientific X-tracta and Qiaquick) and ligated into PCR-Blunt II Topo plasmid (Invitrogen Zero Blunt PCR Cloning Kit), transformed, purified and sequenced (Eton Bioscience). Inserts were digested, purified, and quick-ligated (NEB, cat#M2200S) into the eGFP vector. Resulting clones were verified by digestion and sequencing. DNA was purified (Qiagen spin miniprep kit, cat#27106), and concentration and purity were determined (Nanodrop) before use in transient transfections.

Cell Culture. Stable YFP-H2B expressing HeLa cells (gift from Jagesh Shah, Harvard Medical School), YFP-H3.1 expressing HeLa cells (gift from Ben Black, University of Pennsylvania), HeLa cells (gift from Beth Weaver, University of Wisconsin),143b osteosarcoma cells (gift from Haig Kazazian, University of Pennsylvania), H2AX wild-type and null MEFs [gifts from André Nussenzweig, NIH, (6)] and GM3491 normal human diploid skin fibroblasts (gift from York Marahrens, University of Minnesota) were cultured in DMEM + nonessential amino acids, penicillin-streptomycin, 10% FBS at 37 °C with 5% CO_2.

P175 and P175-NH cells carrying *Sce*I sites (gift from Matt Thayer, Oregon Health Sciences University) were maintained as described (7). TM815 (mouse NIH2/4) cells carrying SceI sites were maintained as described (8). Parental and NHEJ-deficient (Ku86$^{+/-}$ and DNA-PKcs$^{-/-}$ cell lines) HCT116 cells (gift from Eric Hendrickson,University of Minnesota) were maintained as described (9, 10). LigaseIV$^{-/-}$cells were a generous gift from Sehyun Oh and Eric Hendrickson, generated using a Neo-containing rAAV targeting to disrupt the first 302 bp of coding sequence in the first allele, followed by treatment with Cre recombinase and a second round of targeting, as described (11).

Transient Transfection of GFP-Tagged Expression Constructs. Cells were transfected in suspension using Lipofectamine 2000 in Optimem (Invitrogen), plated on fibronectin-coated glass-bottom dishes (see *Sample Preparation*) and incubated overnight. Media with serum was added (McCoy's 5A for HCT116; DMEM for HeLa) a minimum of 1 h before laser exposure. Plasmids encoding GFP-tagged NAC proteins CENP-N, CENP-U, CENP-T, and CENP-M were a gift from Dan Foltz (12). GFP-Ligase IV was a gift from David Chen's lab (University of Texas, Southwestern). The R278H mutation was introduced into this construct using Quickchange (Stratagene), verified by digestion [the mutation creates an *Nde*I site, (13)] and confirmed by sequencing. mCherry-Ligase IV WT and R278H were constructed by replacing the GFP ORF with that of mCherry. These constructs were also verified by digestion and sequencing.

Induction of Double-Strand Breaks by I-*Sce*I. The synthetic glucocorticoid ligand triamcinolone acetonide (TA, Sigma) was dissolved in DMSO. To induce cleavage, human P175 or P175-NH cells (7) were transiently transfected with RFP-SceI-GR using Lipofectamine LTX in Optimem (Invitrogen). Twenty-four hours after transfection, TA was diluted in Optimem (final concentration 10^{-7} M), and this media was added to the transfected cells on the microscope stage (Olympus FV-1000 confocal microscope).

The mouse NIH 2/4 stable cell line (8) was transfected using the Nucleofector kit (Amaxa, Nucleofector R) with the appropriate DNA plasmids, and the fluorescent proteins were visualized 16 h later (Zeiss Meta confocal microscope). Transfection with the RFP–I*Sce*I–GR chimera was performed in cells cultured in DMEM supplemented with 10% stripped serum (Tet system approved; Clontech) and the concentration of triamcinolone acetonide (TA, Sigma) added was 10^{-7} M. For immunofluorescence detection, cells were fixed and H2AX phosphorylation was detected as described (8).

Colony Formation Assays. Cells were plated in triplicate (500,000 cells per well) in 6-well dishes (without fibronectin), and cells were irradiated at 0 Gy, 2 Gy, and 8Gy. Immediately after irradiation, each well was trypsanized and replated into a 10-cm^2 dish. Cells were incubated 10 days under normal culture conditions. Cells were fixed in 100% methanol and stained with 0.2% crystal violet (Sigma cat# C-2886), washed with tap water and allowed to dry; colonies were counted by visual inspection. Standard deviations were calculated using Prism (GraphPad Software).

Immunofluorescence and Confocal Image Collection. After laser exposure, cells in glass-bottom dishes were fixed with 4% formaldehyde for 10′ at room temperature. Mouse anti-H2AX-ser139-P (Upstate, 1:1,000), Chk2-T68P (Cell Signaling, cat#2661, 1:200), hACA (83JD, a gift from Kevin Sullivan, 1:500), anti-Nbs1-Ser-343-P and anti-53BP1 (Calbiochem, a gift from Kevin Harvey, 1:100). Highly cross-absorbed secondary antibodies labeled with Tritc or Cy5 (Jackson); Alexa 488 (Invitrogen) were used at 1:100. Antibodies were diluted in blocking solution (5% serum in PBS + 0.1% Triton X-100) and staining was performed as described (14). Samples were post-fixed with formaldehyde and stored in PBS + 0.1% azide. Confocal microscopy was performed on an Olympus FV-1000.

Automated Microscopy Analysis of Cell Cycle and Cell Death. Live cells in 96-well dishes were exposed to ionizing radiation and then stained with 5 μM Hoechst 33342 (Molecular Probes, cat#H-3570, 3,000× stock solution) diluted in PBS, and images were collected using the Cellomics ArrayScan (ThermoFisher) Target Activation module with a 20× Zeiss lens, five fields per well (a minimum of 2,500 cells per well), three wells per sample. Object identification used automated segmentation of Hoechst. Analysis used custom software (CellFinder, based on the DataGraph framework,http://www.visualdatatools.com/DataGraph/) to generate scatterplots for subset quantitation. For apoptosis quantitation (Fig. 6*C*), cells in the brightest subset of Hoechst signal (total intensity >100,000) were counted relative to total cell numbers, and percentages and standard deviations were calculated using Prism (GraphPad Software). Similar methods were used to measure nuclear area (detected with DAPI) for cell cycle analysis shown in Fig. S3, and further validated by analysis using ImageJ.

1. Sugimoto K, Fukuda R, Himeno M (2000) Centromere/kinetochore localization of human centromere protein A (CENP-A) exogenously expressed as a fusion to green fluorescent protein. *Cell Struct Funct* 25:253–261.
2. Botvinick EL, Berns MW (2005) Internet-based robotic laser scissors and tweezers microscopy. *Microsc Res Tech* 68:65–74.
3. Kong X, et al. (2009) Comparative analysis of different laser systems to study cellular responses to DNA damage in mammalian cells. *Nucleic Acids Res.*

4. Shelby RD, Vafa O, Sullivan KF (1997) Assembly of CENP-A into centromeric chromatin requires a cooperative array of nucleosomal DNA contact sites. *J Cell Biol* 136:501–513.
5. Black BE, et al. (2004) Structural determinants for generating centromeric chromatin. *Nature* 430:578–582.
6. Celeste A, et al. (2003) Histone H2AX phosphorylation is dispensable for the initial recognition of DNA breaks. *Nat Cell Biol* 5:675–679.
7. Breger KS, Smith L, Thayer MJ (2005) Engineering translocations with delayed replication: evidence for cis control of chromosome replication timing. *Hum Mol Genet* 14:2813–2827.
8. Soutoglou E, et al. (2007) Positional stability of single double-strand breaks in mammalian cells. *Nat Cell Biol* 9:675–682.
9. Li G, Nelsen C, Hendrickson EA (2002) Ku86 is essential in human somatic cells. *Proc Natl Acad Sci USA* 99:832–837.
10. Ruis BL, Fattah KR, Hendrickson EA (2008) The catalytic subunit of DNA-dependent protein kinase regulates proliferation, telomere length and genomic stability in human somatic cells. *Mol Cell Biol* 28:6182–6195.
11. Kohli M, Rago C, Lengauer C, Kinzler KW, Vogelstein B (2004) Facile methods for generating human somatic cell gene knockouts using recombinant adeno-associated viruses. *Nucleic Acids Res* 32:e3.
12. Foltz DR, et al. (2006) The human CENP-A centromeric nucleosome-associated complex. *Nat Cell Biol* 8:458–469.
13. Riballo E, et al. (1999) Identification of a defect in DNA ligase IV in a radiosensitive leukaemia patient. *Curr Biol* 9:699–702.
14. Zeitlin SG, Barber CM, Allis CD, Sullivan KF (2001) Differential regulation of CENP-A and histone H3 phosphorylation in G2/M. *J Cell Sci* 114:653–661.

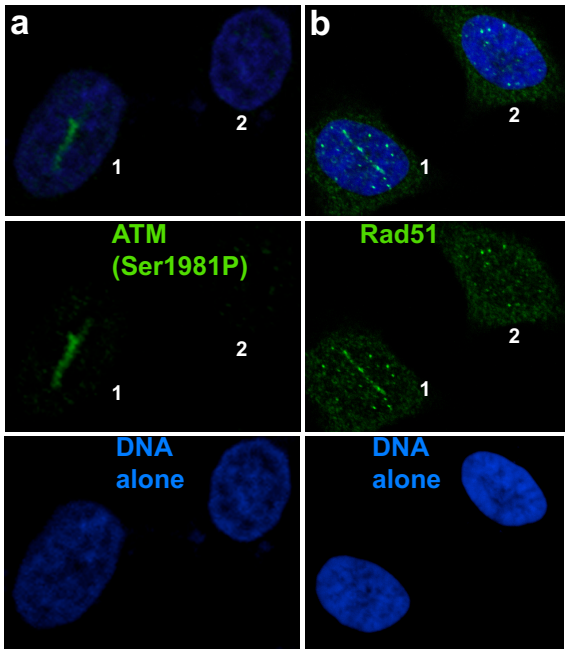

Fig. S1. Laser targeting activates ATM and recruits Rad51. Immunofluorescence detection of markers for double-strand breaks. HeLa cells were exposed (cell #1) or not exposed (cell #2) to laser targeting, fixed and incubated with antibodies to detect activated (phosphorylated at Ser-1981) ATM kinase (*a*) or for Rad51 (*b*), shown in green. DNA (detected with DAPI) is shown in blue).

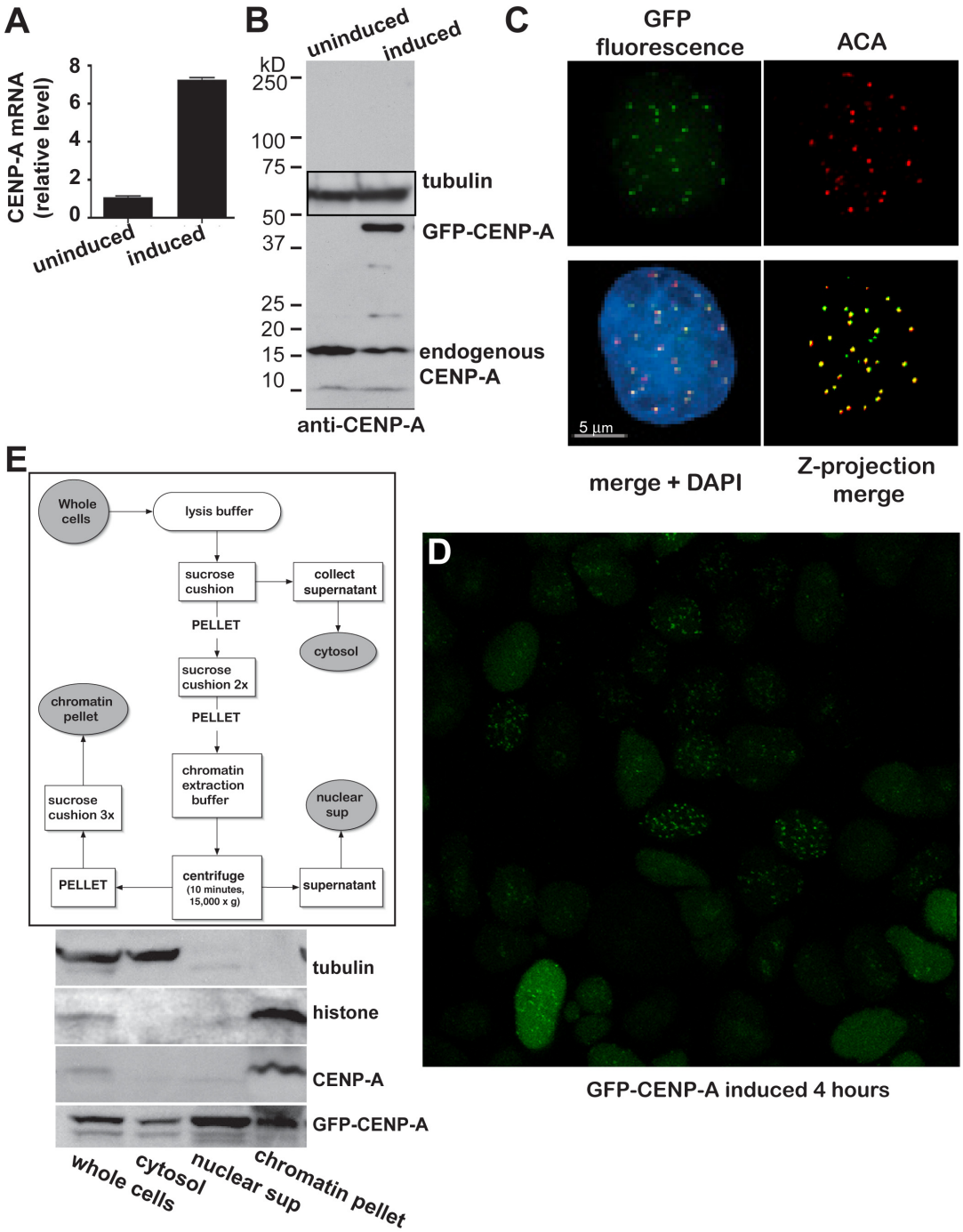

Fig. S2. Characterization of inducible GFP-CENP-A cell lines. (*A*) Relative levels of CENP-A mRNA before (uninduced) and after addition of tetracycline (induced) were measured using quantitative RT-PCR. (*B*) Relative levels of tagged and endogenous CENP-A protein were measured by western analysis with an antibody that detects both proteins with and without tetracycline induction. Tubulin was detected as a loading control. (*C*) Colocalization of GFP-CENP-A fluorescence [previously characterized (1)] with endogenous centromeres (detected with human autoimmune anti-centromere antisera, hACA, in red) was assessed using single confocal slices. DNA is detected with DAPI and shown in blue. Since GFP-CENP-A and hACA levels are not always equal, a Z-projection is shown (far right) where levels were equalized to emphasize overlap (yellow). (*D*) Variable pattern of GFP-CENP-A localization at early timepoints after induction is shown in an example confocal image. Similar results were obtained with multiple clonal cell lines. (*E*) The majority of endogenous CENP-A (anti-CENP-A) and core histone fraction (anti-H3 antibody) are tightly bound to DNA, since these remain in the chromatin subfraction (chr) after washing with high salt and detergent. Approximately equal quantities of GFP-CENP-A (anti-GFP) are detected in both a nuclear fraction extracted by high salt and detergent (nuclear sup) and an insoluble fraction (chromatin pellet).

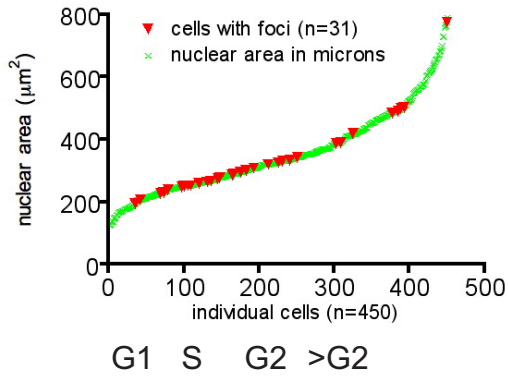

Fig. S3. Nuclear size analysis of cell cycle stage distribution of cells displaying CENP-A focus formation. A dish of cells exposed to laser targeting was fixed with formaldehyde, and DNA was detected with DAPI. Images were collected on a population of cells, and nuclear areas were calculated for this population (green ×s). The nuclear areas of cells with GFP-CENP-A foci were mapped onto this distribution (red triangles).

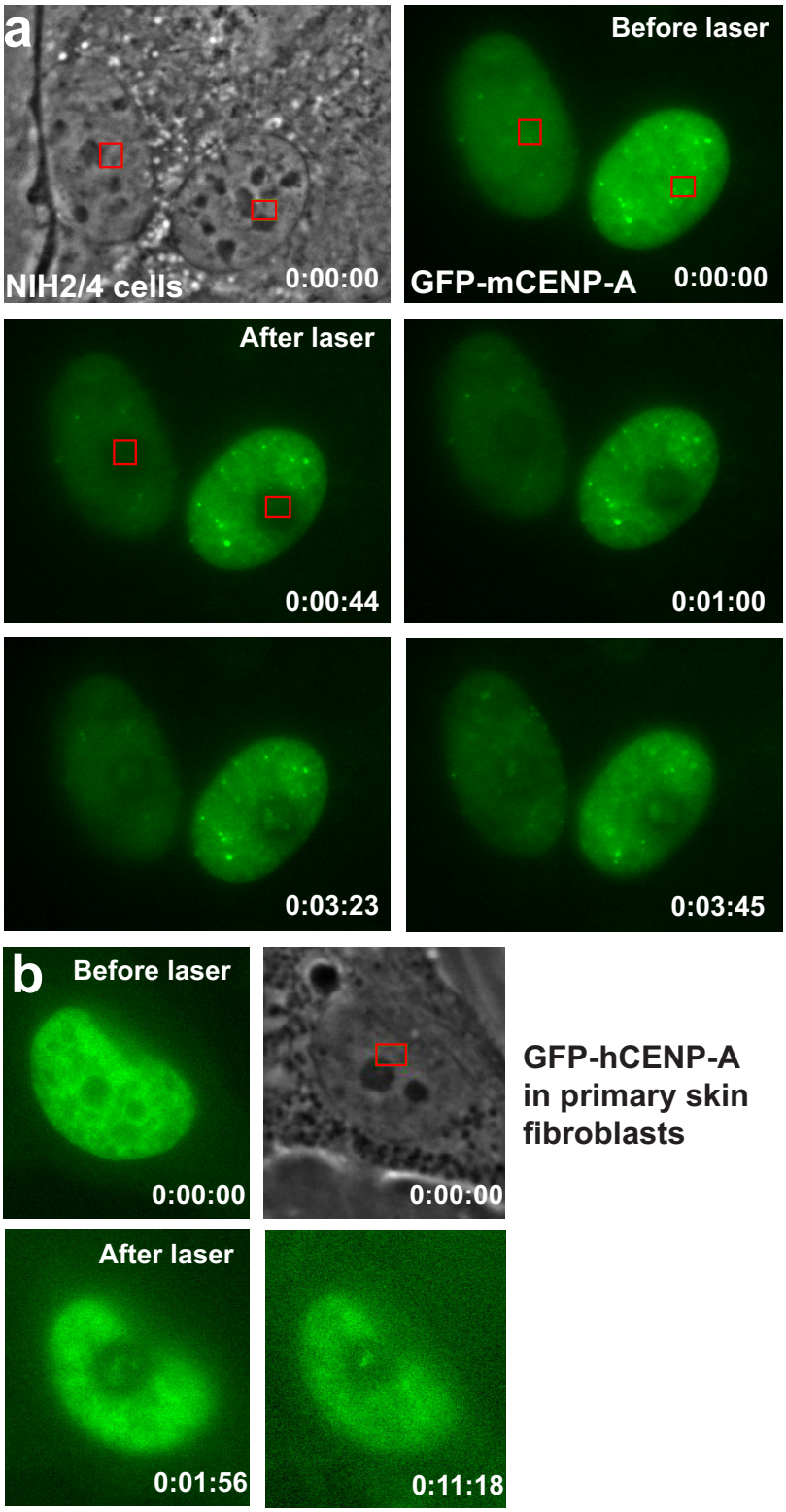

Fig. S4. GFP-tagged mouse CENP-A accumulates in areas of laser-induced DNA damage in mouse cells, and GFP-tagged human CENP-A behaves similarly in primary human cells. (*a*) GFP-tagged mouse CENP-A was transiently transfected into NIH 2/4 cells, and these cells were subjected to laser exposure. (*b*) GFP-tagged human CENP-A was transiently transfected into primary human GM3491 cells, and these cells were subjected to laser exposure. Timestamp represents hours:minutes:seconds.

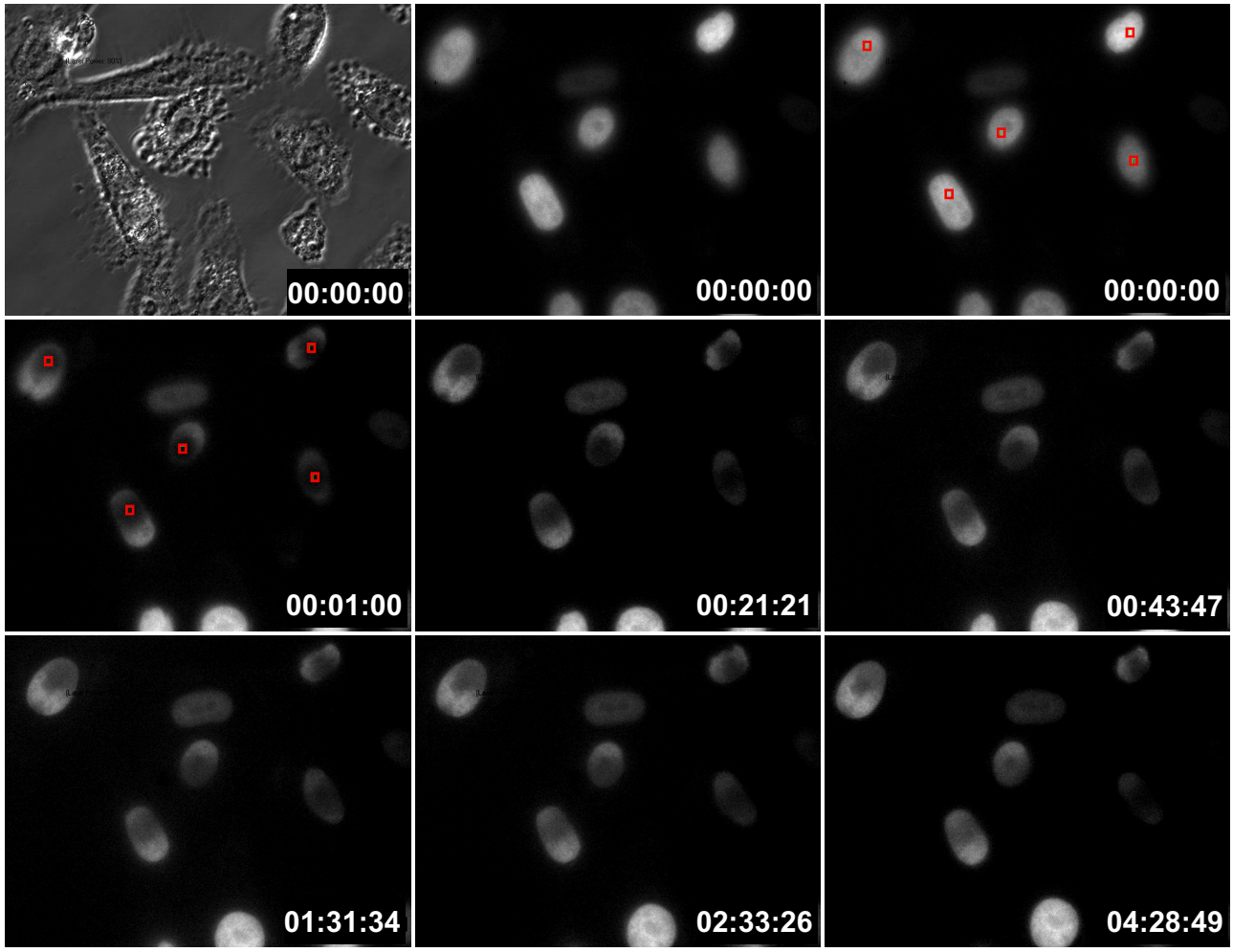

YFP-H3.1 (HeLa stable cell line)

Fig. S5. Example extended timelapse of YFP-H3.1 recovery after laser targeting. Targeted areas are shown in red. Timestamp is shown in hours:minutes:seconds. YFP is shown in grayscale.

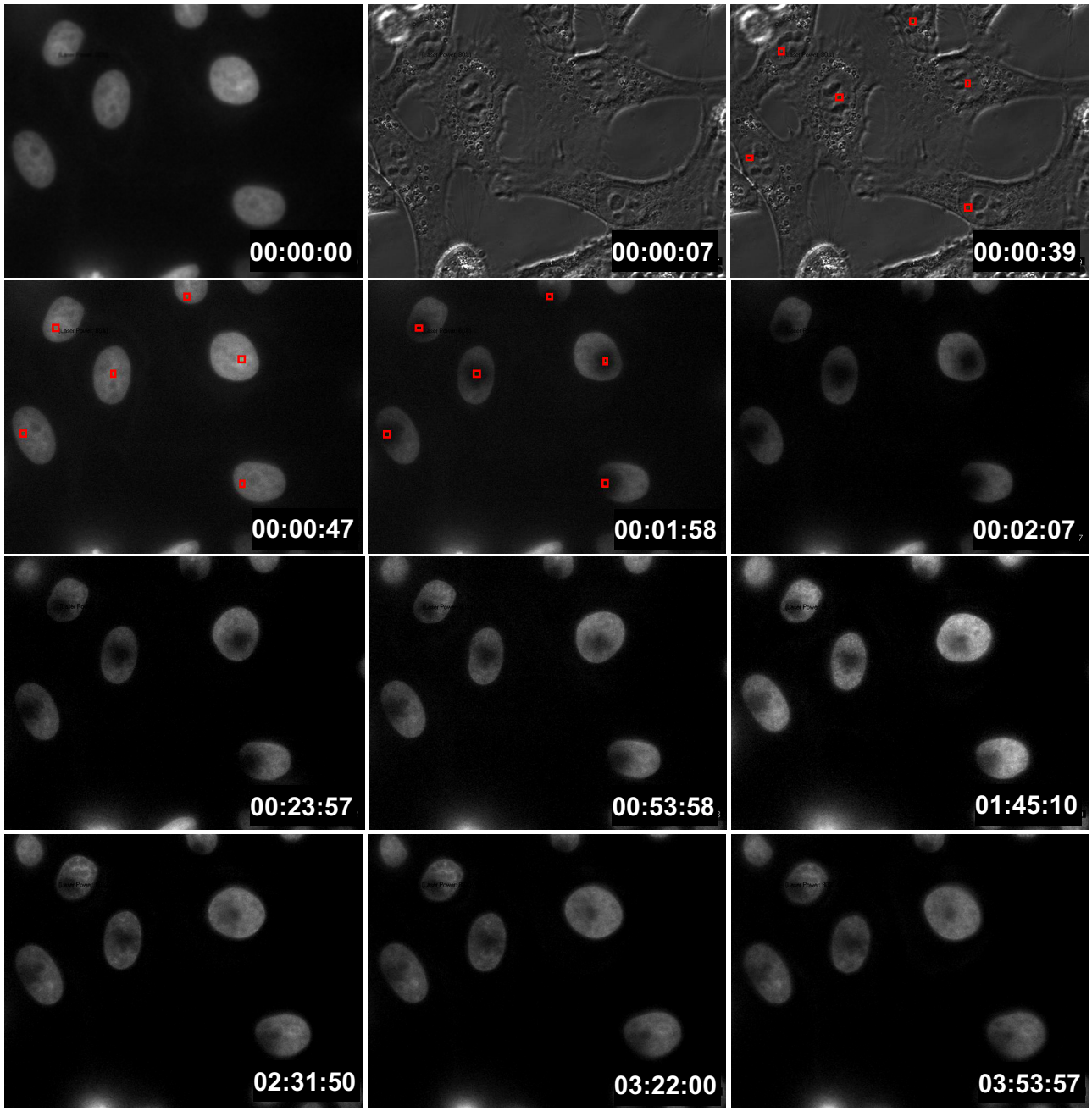

YFP-H2B (HeLa stable cell line)

Fig. S6. Example extended timelapse of YFP-H2B recovery after laser targeting. Targeted areas are shown in red. Timestamp is shown in hours:minutes:seconds. YFP is shown in grayscale.

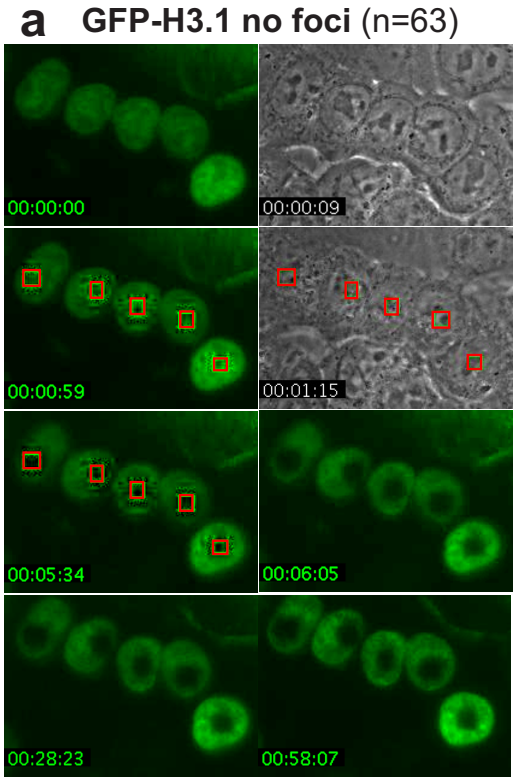

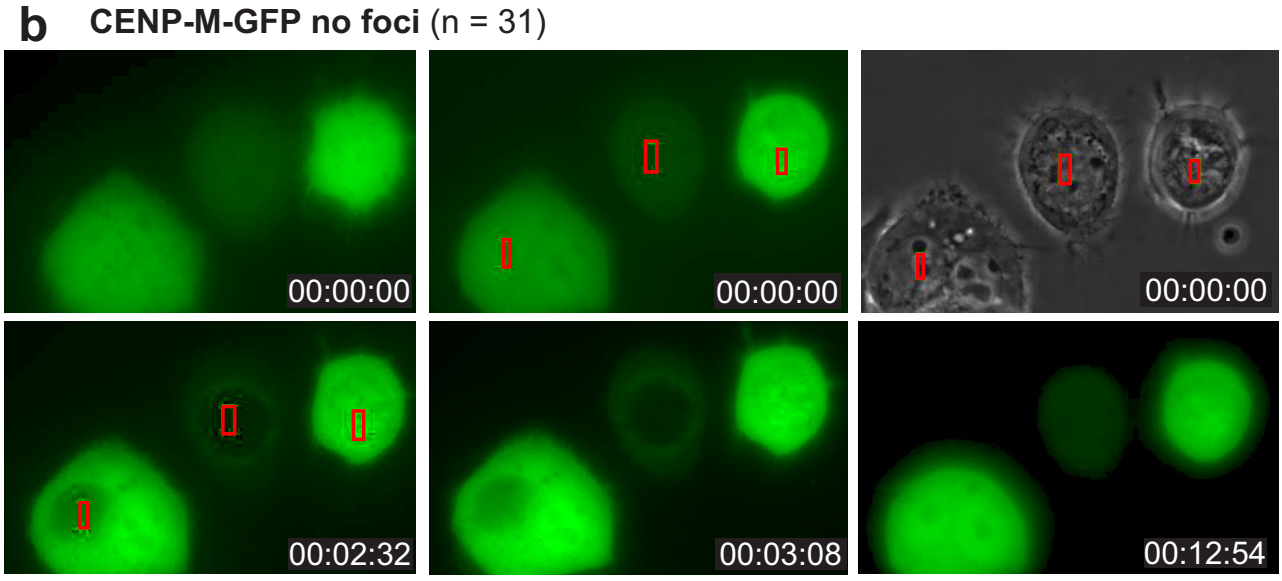

Fig. S7. No focal accumulations in cells transiently transfected to overexpress GFP-H3.1 or GFP-CENP-M. (*a*) Example images from transient transfections of GFP-H3.1 expression plasmid in HCT116 cells. No accumulations were observed in areas of laser targeting (red boxes). (*b*) GFP-CENP-M nuclear fluorescence bleached extensively but recovered rapidly, although accumulation at the site of laser targeting was not observed (n = 31 cells). Timestamp represents hours:minutes:seconds.

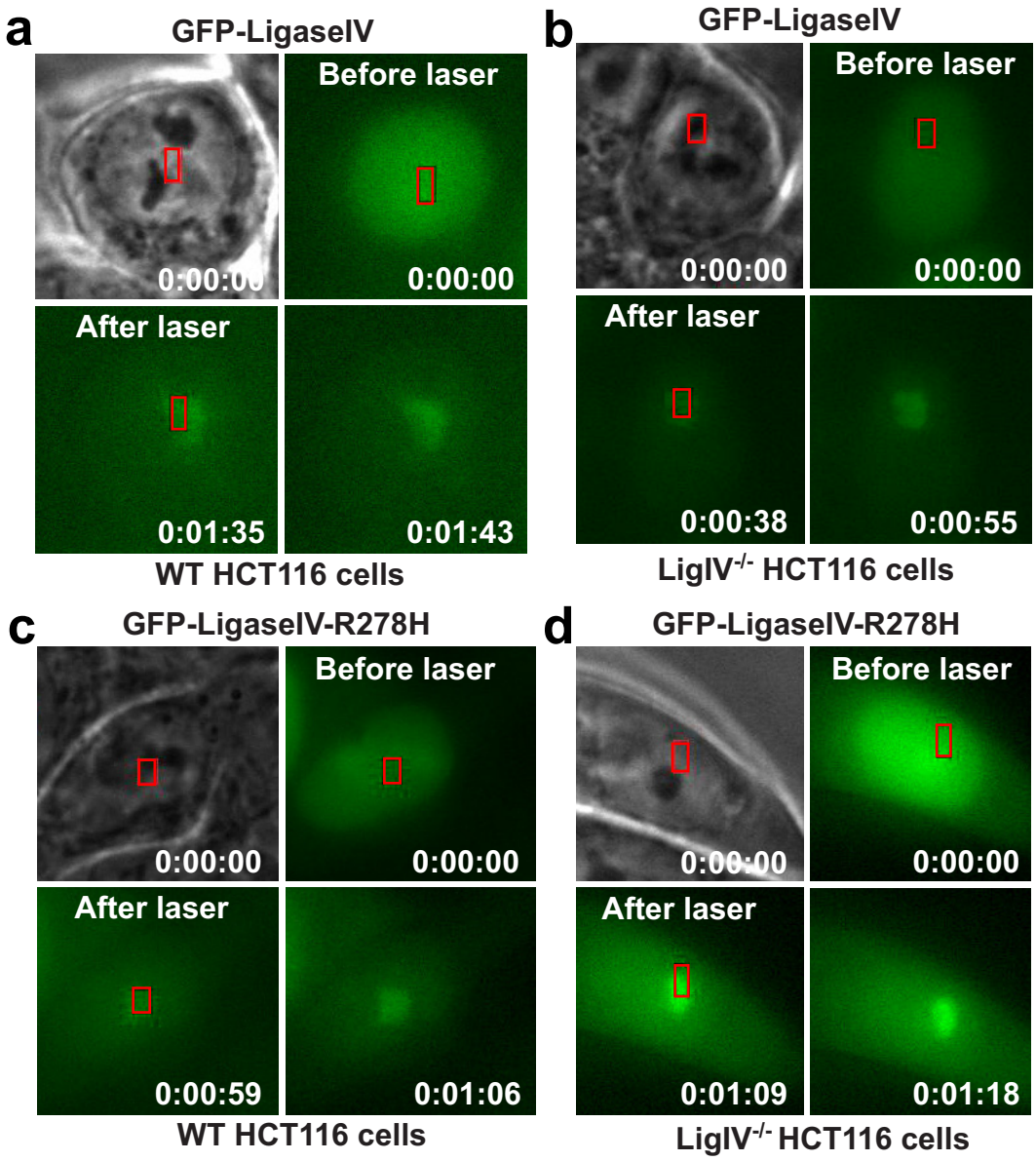

Fig. S8. Ligase IV recruitment to sites of laser-induced DNA damage. GFP-LigaseIV focus formation after laser exposure in WT (*a*) or LigaseIV$^{-/-}$ (*b*) HCT116 cells. GFP-LigaseIV-R278H focus formation after laser exposure in WT (*c*) or LigaseIV$^{-/-}$ (*d*) HCT116 cells. Timestamp represents hours:minutes:seconds.

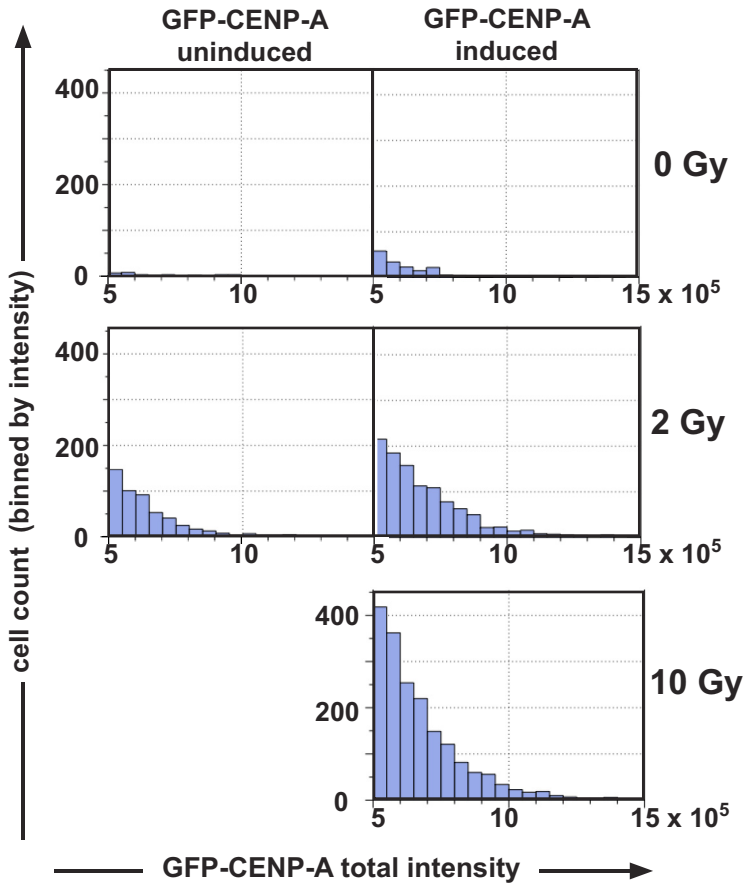

Fig. S9. GFP-CENP-A-positive cells accumulate, and GFP fluorescence levels increase, transiently after radiation-induced DNA damage. Population analysis demonstrated that GFP-CENP-A signals increased transiently after irradiation in a dose-dependent manner, suggesting post-translational stabilization of GFP-CENP-A protein in response to DNA damage.